Challa S. S. R. Kumar *Editor*

UV-VIS and Photoluminescence Spectroscopy for Nanomaterials Characterization

Springer

UV-VIS and Photoluminescence Spectroscopy for Nanomaterials Characterization

Challa S.S.R. Kumar
Editor

UV-VIS and Photoluminescence Spectroscopy for Nanomaterials Characterization

With 278 Figures and 5 Tables

Springer

Editor
Challa S.S.R. Kumar
Center for Advanced Microstructures and Devices
Baton Rouge, LA, USA

ISBN 978-3-642-27593-7 ISBN 978-3-642-27594-4 (eBook)
DOI 10.1007/978-3-642-27594-4
Springer Heidelberg New York Dordrecht London

Library of Congress Control Number: 2013930307

Printed on acid-free paper

Springer is part of Springer Science + Business Media (www.springer.com)

Editor-in-Chief

Challa S.S.R. Kumar
Center for Advanced Microstructures and Devices
Baton Rouge, LA
USA

Contents

List of Contributors

Michael M. Adachi Department of Electrical and Computer Engineering, University of Waterloo, Waterloo, ON, Canada

X. Y. Chen Department of Physics, The University of Hong Kong, Pokfulam Road, Hong Kong

Rui Chen Division of Physics and Applied Physics, School of Physical and Mathematical Sciences, Nanyang Technological University, Singapore, Singapore

Mircea Cotlet Brookhaven National Laboratory, Upton, NY, USA

Masih Darbandi Faculty of Physics and Center for Nanointegration Duisburg-Essen (CeNIDE), University of Duisburg-Essen, Duisburg, Germany

Hilmi Volkan Demir Department of Electrical and Electronics Engineering, Department of Physics and UNAM—Institute of Materials Science and Nanotechnology, Bilkent University, Ankara, Turkey

Luminous! Centre of Excellence for Semiconductor Lighting and Displays, School of Electrical and Electronic Engineering, School of Physical and Mathematical Sciences, Nanyang Technological University, Singapore, Singapore

A. B. Djurišić Department of Physics, The University of Hong Kong, Pokfulam Road, Hong Kong

Ricardo M. Abraham Ekeroth Grupo de Óptica de Sólidos-Elfo, Centro de Investigaciones en Física e Ingeniería del Centro de la Provincia de Buenos Aires – Instituto de Física Arroyo Seco, Facultad de Ciencias Exactas, Universidad Nacional del Centro de la Provincia de Buenos Aires, Buenos Aires, Argentina

Consejo Nacional de Investigaciones Científicas y Técnicas CONICET, Buenos Aires, Argentina

Hao Jing Department of Chemistry and Biochemistry, University of South Carolina, Columbia, SC, USA

Karim S. Karim Department of Electrical and Computer Engineering, University of Waterloo, Waterloo, ON, Canada

Mohammedreza Khorasaninejad Department of Electrical and Computer Engineering, University of Waterloo, Waterloo, ON, Canada

Jae-Seung Lee Department of Materials Science and Engineering, Korea University, Seoul, Republic of Korea

Marcelo Lester Grupo de Óptica de Sólidos-Elfo, Centro de Investigaciones en Física e Ingeniería del Centro de la Provincia de Buenos Aires – Instituto de Física Arroyo Seco, Facultad de Ciencias Exactas, Universidad Nacional del Centro de la Provincia de Buenos Aires, Buenos Aires, Argentina

Consejo Nacional de Investigaciones Científicas y Técnicas CONICET, Buenos Aires, Argentina

Y. H. Leung Department of Physics, The University of Hong Kong, Pokfulam Road, Hong Kong

Dehui Li Division of Physics and Applied Physics, School of Physical and Mathematical Sciences, Nanyang Technological University, Singapore, Singapore

A. M. C. Ng Department of Physics, The University of Hong Kong, Pokfulam Road, Hong Kong

Nanostructure Institute for Energy and Environmental Research, Division of Physical Sciences, South University of Science and Technology of China, Shenzhen, China

Timothy O'Connor Department of Physics, Bowling Green State University, Bowling Green, USA

Kenji Okitsu Graduate School of Engineering, Osaka Prefecture University, Naka-ku, Sakai, Osaka, Japan

Umapada Pal Instituto de Física, Benemérita Universidad Autónoma de Puebla, Puebla, Puebla, Mexico

Ovidio Peña-Rodríguez Centro de Microanálisis de Materiales (CMAM), Universidad Autónoma de Madrid (UAM), Madrid, Spain

Instituto de Óptica, Consejo Superior de Investigaciones Científicas (IO-CSIC), Madrid, Spain

Simarjeet S. Saini Department of Electrical and Computer Engineering, University of Waterloo, Waterloo, ON, Canada

Jesica M. J. Santillán Centro de Investigaciones Ópticas (CIOp), CONICET La Plata-CIC, La Plata, Argentina

Departamento de Ciencias Básicas, Facultad de Ingeniería, Universidad Nacional de La Plata, La Plata, Argentina

Lucía B. Scaffardi Centro de Investigaciones Ópticas (CIOp), CONICET La Plata-CIC, La Plata, Argentina

Departamento de Ciencias Básicas, Facultad de Ingeniería, Universidad Nacional de La Plata, La Plata, Argentina

Daniel C. Schinca Centro de Investigaciones Ópticas (CIOp), CONICET La Plata-CIC, La Plata, Argentina

Departamento de Ciencias Básicas, Facultad de Ingeniería, Universidad Nacional de La Plata, La Plata, Argentina

Urartu Özgür Şafak Şeker Department of Electrical and Electronics Engineering, Department of Physics and UNAM—Institute of Materials Science and Nanotechnology, Bilkent University, Ankara, Turkey

Luminous! Centre of Excellence for Semiconductor Lighting and Displays, School of Electrical and Electronic Engineering, School of Physical and Mathematical Sciences, Nanyang Technological University, Singapore, Singapore

Handong Sun Division of Physics and Applied Physics, School of Physical and Mathematical Sciences, Nanyang Technological University, Singapore, Singapore

J. Toudert Instituto de Optica, CSIC, Madrid, Spain

Pol Van Dorpe imec vzw, Leuven, Belgium

Physics Department, KU Leuven, Leuven, Belgium

Fabián A. Videla Centro de Investigaciones Ópticas (CIOp), CONICET La Plata-CIC, La Plata, Argentina

Departamento de Ciencias Básicas, Facultad de Ingeniería, Universidad Nacional de La Plata, La Plata, Argentina

Moriaki Wakaki Department of Optical and Imaging Science & Technology, School of Engineering, Tokai University, Hiratsuka, Kanagawa, Japan

Hui Wang Department of Chemistry and Biochemistry, University of South Carolina, Columbia, SC, USA

Qihua Xiong Division of Physics and Applied Physics, School of Physical and Mathematical Sciences, Nanyang Technological University, Singapore, Singapore

Division of Microelectronics, School of Electrical and Electronics Engineering, Nanyang Technological University, Singapore, Singapore

Zhihua Xu Department of Chemical Engineering, University of Minnesota Duluth, Duluth, MN, USA

Jian Ye imec vzw, Leuven, Belgium

Chemistry Department, KU Leuven, Leuven, Belgium

Eisuke Yokoyama Department of Optical and Imaging Science & Technology, School of Engineering, Tokai University, Hiratsuka, Kanagawa, Japan

Mikhail Zamkov Department of Physics, Bowling Green State University, Bowling Green, USA

J. A. Zapien Department of Physics and Materials Science, City University of Hong Kong, Kowloon, Hong Kong

Li Zhang Department of Chemistry and Biochemistry, University of South Carolina, Columbia, SC, USA

Geometrically Tunable Optical Properties of Metal Nanoparticles

1

Hao Jing, Li Zhang, and Hui Wang

Contents

H. Jing • L. Zhang • H. Wang (✉)
Department of Chemistry and Biochemistry, University of South Carolina, Columbia, SC, USA

Challa S.S.R. Kumar (ed.), *UV-VIS and Photoluminescence Spectroscopy for Nanomaterials Characterization*, DOI 10.1007/978-3-642-27594-4_1,

1 Definition of the Topic

Noble metal nanoparticles exhibit fascinating geometrically tunable optical properties that are dominated by their localized surface plasmon resonances (LSPRs). By judiciously tailoring the geometric parameters of a metal nanoparticle, one can fine-tune the nanoparticle's optical responses in a precisely controllable manner and thereby selectively implement desired optical properties into nanomaterial systems or nanodevices for specific applications. In this chapter, we present a review on the recent experimental and theoretical advances in the understanding of the geometry–optical property relationship of metallic nanoparticles in various geometries.

2 Overview

Metal nanoparticles are an important class of subwavelength optical components whose optical properties can be fine-tuned over a broad spectral range by tailoring their geometric parameters. The fascinating optical characteristics of metallic nanoparticles are essentially determined by the collective oscillations of free electrons in the metals, known as plasmons. Metallic nanostructures possess geometry-dependent localized surface plasmon resonances, which has stimulated growing interests in a rapidly expanding array of metallic nanoparticle geometries, such as nanorods, nanoshells, nanoprisms, nanostars, and nanocages. The resonant excitation of plasmons also leads to large enhancements of the local electromagnetic field in close proximity to the nanoparticle surface, resulting in dramatically enhanced cross sections for nonlinear optical spectroscopies such as surface-enhanced Raman scattering. These highly tunable plasmonic properties of metal nanoparticles allow for the development of fundamentally new metal-based subwavelength optical elements with broad technological potential, an emerging field known as plasmonics.

The past decades have witnessed significant advances in scientific understanding of the origin of the optical tunability of metallic nanoparticle systems, primarily driven by the rapid advances in the geometry-controlled nanoparticle fabrication and assembly and electrodynamics modeling of nanoparticle systems. In this chapter, we present a state-of-the-art review on the geometrically tunable plasmonic properties of metallic nanostructures in various geometries. We describe, both experimentally and theoretically, the relationship between the particle geometry and optical properties in a series of nanoparticle geometries, including

strongly coupling multi-nanoparticle systems, to demonstrate how the optical responses of a nanoparticle can be fine-tuned by judiciously tailoring the geometric parameters of the particle and how the tunable optical properties can be used to tackle grand challenges in diverse fields, such as photonics, energy conversion, spectroscopies, molecular sensing, and biomedicine.

3 Introduction

Nanoparticles exhibit a whole set of fascinating size- and shape-dependent physical and chemical properties that are dramatically different from those of either the corresponding bulk materials or the atomic and molecular systems [1]. Nanoparticles of noble metals, such as Au, Ag, and Cu, have attracted tremendous attention due to their interesting geometry-dependent optical properties. Actually, the vivid, beautiful color of colloidal metal nanoparticles has been an object of fascination since ancient times. One of the oldest examples is the famous Lycurgus Cup (Byzantine Empire, fourth century AD) (Fig. 1.1). This glass cup shows a striking red color when light is shone into the cup and transmitted through the glass, while viewed in reflected light, it appears green. This peculiar behavior is essentially due to the small Au–Ag bimetallic nanoparticles embedded in the glass, which show a strong optical absorption of light in the green part of the visible spectrum.

While these optical characteristics of metal colloids have been known and used for centuries, our scientific understanding on the origin of these properties has emerged far more recently, beginning with the development of classical electromagnetic theory. About a century ago, Gustav Mie applied Maxwell's equations to explain the strong absorption of green light by a Au nanosphere under plane wave illumination [2], which established, for the first time, the rigorous scientific foundation for our understanding of this interesting phenomenon. Essentially, the fascinating optically resonant behaviors of metal nanoparticles are determined by the collective oscillations of free electrons in the metals, known as plasmons. A plasmon resonance can be optically excited when a photon is absorbed at the metal–dielectric interface and transfers the energy into the collective electron oscillations, which are coupled in-phase with the incident light at a certain resonant frequency. For metal nanoparticles, the plasmon resonance frequencies are dependent upon the size and shape of the nanoparticles as the oscillations of free electrons are confined by the particle boundaries over finite nanoscale dimensions. It is well-known that solid spherical Au nanoparticles of ~30 nm in diameter strongly absorb green light at ~520 nm when their characteristic dipole plasmon resonance is optically excited, giving rise to a deep red color when dispersed in colloidal solutions. Michael Faraday was the first person to observe this spectacular phenomenon [3]. In 1857, he prepared the first stable suspension of Au colloids by reducing gold chloride with phosphorus in water. Some of his original samples are still well preserved and on display at the Faraday Museum in London.

The past two decades have witnessed rapid advances in the geometry-controlled fabrication of metallic nanostructures and electrodynamics simulation of the

Fig. 1.1 Pictures of the Lycurgus Cup (on display in the British Museum)

nanoparticles' optical properties, which allow for the development of quantitative understanding of the structure–property relationship of a series of metallic nanoparticle geometries with increasing structural complexity. It has become increasingly apparent that by adjusting the geometric parameters of metal nanostructures, one can fine-tune the wavelengths at which the nanoparticles interact with the incident light in a highly precise manner [1, 4–8]. The plasmon resonance frequencies of a metal nanoparticle are not only a function of the electronic properties of the constituent metal and the dielectric properties of the surrounding medium but also, especially on the nanometer-length scale, more sensitively dependent upon the size and shape of the particle. It is of paramount importance to create highly tunable plasmon resonances of nanoparticles over a broad spectral range because it can open a whole set of new opportunities for photonic, optoelectronic, spectroscopic, and biomedical applications. For example, expanding the plasmonic tunability of metallic nanoparticles from the visible into the near-infrared (NIR) "water window" where tissues and blood are relatively transparent provides unique opportunities for the integrated high-contrast cancer imaging and high-efficiency photothermal therapy [9, 10]. This has, in turn, stimulated tremendous interests in a rapidly expanding array of metal nanoparticle geometries, such as nanorods [11–16] nanoprisms [17–21], nanoshells [22–24] nanostars [25, 26], and nanocages [27, 28]. A key feature of these nanostructures is that their plasmon resonances are geometrically tunable, which enables one to set the plasmon resonances at a specific laser wavelength or spectral region that match a particular application.

In this chapter, we present a comprehensive review on the geometrically tunable optical properties of metal nanostructures. In Sect. 4, we give a brief introduction to the fundamentals of plasmon resonances supported by metal nanoparticles, covering both the experimental measurements and the theoretical methods for plasmon modeling. In Sect. 5, we start from the optical properties of the simplest geometry, solid metal nanospheres, to discuss how the free carrier density of the materials, the electronic properties of metals, and the size of spherical particles determine the

particles' overall optical properties. We also talk about the optical tunability of bimetallic heterostructured and alloy nanospheres. In Sects. 6 and 7, we focus on two representative nanoparticle geometries, nanorods and nanoshells, respectively, to demonstrate how various geometric parameters determine the plasmon-dominated optical properties of the nanoparticles with a particular focus on fundamental understanding of the origin of the optical tunability in these nanoparticle geometries. Essentially, the frequencies of plasmon resonances of metallic nanorods are determined by the aspect ratio of the nanorods, whereas the highly tunable nanoshell LSPRs arise from the interactions between the plasmon modes supported by the inner- and outer-shell surfaces. In Sect. 8, we give a brief survey of the structure–property relationships of several representative nanoparticle geometries with anisotropic structures, such as nanoprisms, nanopolyhedra, nanostars, and nanocages. In Sect. 9, we set out to talk about the geometrically tunable optical properties of more complicated multi-nanoparticle systems in which strong plasmon coupling occurs. We particularly emphasize on how the plasmonic interactions between nanoparticle building blocks give rise to the hybridized plasmon modes of the multiparticle systems and further enhanced local fields in the interparticle junctions that are exploitable for surface-enhanced spectroscopies. Finally, in Sect. 10, we summarize the latest progress in nanoparticle plasmonics over the past two decades and briefly comment on how the geometrically tunable LSPRs of metal nanoparticle systems will broadly impact the fundamental research on nanophotonics and technological applications of metal nanostructures.

4 Localized Surface Plasmon Resonances (LSPRs)

4.1 Plasmons: Collective Oscillations of Free Electrons

Early understanding of the theory of nanoparticle plasmons dates back to the work done by Mie [2] and Faraday [3] more than a century ago. In this chapter, it is not intended to thoroughly cover the plasmon theories in detail, since a good number of excellent reviews, such as the books by Kreibig and Vollmer [29] and by Bohren and Huffman [30] as well as review articles by Mulvaney [31] and by El-Sayed [5], have already been published on this topic, and the readers are encouraged to read them for further details. Here we only want to give a brief introduction to the fundamentals of plasmon resonances of metal nanoparticles.

Essentially, plasmons arise from the collective oscillations of free electrons in metallic materials. Under the irradiation of an electromagnetic wave, the free electrons are driven by the electric field to coherently oscillate at a plasmon frequency of ω_B relative to the lattice of positive ions [29]. For a bulk metal with infinite sizes in three dimensions in vacuum, ω_B can be expressed as

$$\omega_B = \sqrt{\frac{4\pi e^2 n}{me}} \tag{1.1}$$

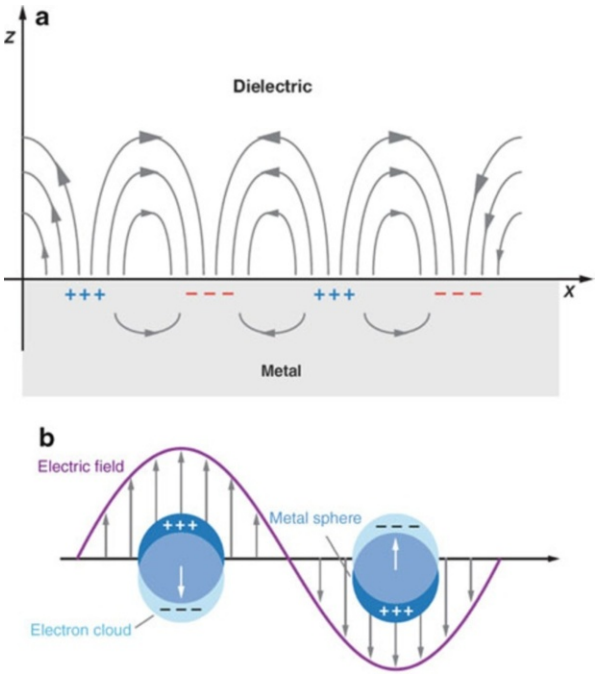

Fig. 1.2 Schematic illustrations of (**a**) a propagating plasmon at metal–dielectric interface and (**b**) a LSPR of a metal nanosphere (Adapted with permission from Ref. [33]. Copyright 2007 Annual Reviews)

where n is the number density of electrons and e and m_e are the charge and effective mass of electrons, respectively.

However, in reality, we have to deal with metallic structures of finite dimensions that are surrounded by materials with different dielectric properties. Since an electromagnetic wave impinging on a metal surface only has a certain penetration depth (~50 nm for Ag and Au), only the electrons on the surface are the most significant. Therefore, their collective oscillations are properly termed as surface plasmons [32]. At a metal–vacuum interface, application of the boundary conditions results in a surface plasmon mode with a frequency $\omega_{surf} = \frac{\omega_p}{\sqrt{2}}$. As is shown in Fig. 1.2a, such a surface plasmon mode represents a longitudinal charge density wave that travels across the surface [33], also widely known as a propagating plasmon. A surface plasmon mode can be excited through a resonance mechanism by passing an electron through a thin metallic film or by reflecting an electron or a photon from the surface of a metallic film when the frequency and wave vectors of both the incident light and the surface plasmon match each other.

In metallic nanoparticle systems, the collective oscillations of free electrons are confined to a finite volume defined by the particle dimensions. Since the plasmons of nanoparticles are localized rather than propagating, they are known as localized surface plasmon resonances (LSPRs). When the free electrons in a metallic nanostructure are driven by the incident electric field to collectively oscillate at a certain resonant frequency, the incident light is absorbed by the nanoparticles. Some of these photons will be released with the same frequency and energy in all directions,

which is known as the process of scattering. Meanwhile, some of these photons will be converted into phonons or vibrations of the lattice, which is referred to as absorption [30]. Therefore, LSPRs manifest themselves as a combined effect of scattering and absorption in the optical extinction spectra. As depicted in Fig. 1.2b, the free electrons of Au nanospheres oscillate coherently in response to the electric field of incident light [33]. The multipolar resonant frequencies can be represented as $\omega_{S.l} = \omega_B \sqrt{\frac{l}{2l+1}}$ (l = 1, 2, 3, 4. . .) when this process occurs in a vacuum. It has been known that the number, location, and intensity of LSPR peaks of Au or Ag nanoparticles are strongly correlated with both the shape and size of the nanoparticles.

4.2 Experimental Methodology of LSPR Measurements

There are generally two important effects associated with the excitation of LSPRs, the existence of optical extinction maxima at the plasmon resonance frequencies (far-field properties) and significantly enhanced electric fields in close proximity to the particle's surface (near-field properties). The far-field plasmonic properties of metal nanoparticles can be most conveniently measured by performing extinction spectroscopy measurements on colloidal nanoparticle suspensions or on thin films of nanoparticles immobilized on or embedded in a substrate at ensemble level using UV–visible–NIR spectrometers. In these measurements, both absorption and scattering contribute to the overall extinction. The polydispersity of the samples may introduce inhomogeneous broadening to the overall bandwidth and modify the line shape of the extinction spectra. To bypass the ensemble-averaging effects, one can use a dark-field microscope coupled with a spectrometer to probe the wavelength-dependent light-scattering properties of individual nanoparticles at single-particle level. Figure 1.3 shows a dark-field microscopy image of Au nanoparticles of different geometries and the corresponding scattering spectra of each individual nanoparticle [34]. The different nanoparticles exhibit dramatically different colors and intensities in the microscopy images and are resonant with the incident light at different wavelengths. By adding linear polarizers and other optical accessories to the dark-field microscope, the spatial distribution of the scattering light at a certain wavelength can be measured. By correlating the optical characteristics probed by dark-field microscopy with the detailed structural information obtained from electron microscopies at single-particle level, one can develop quantitative understanding of the structure–property relationship of individual nanoparticles without the ensemble-averaging effects. Since the electrodynamics simulations are mostly carried out on individual nanoparticles, the single-particle measurements provide unique opportunities to directly compare the experimental spectra to the simulated results.

In addition to the abovementioned far-field measurements, near-field scanning optical microscopy (NSOM) has been applied to the near-field measurements of LSPRs. NSOM is a powerful imaging tool which permits super-resolution imaging of samples through the interaction of the light with the samples close to the metal

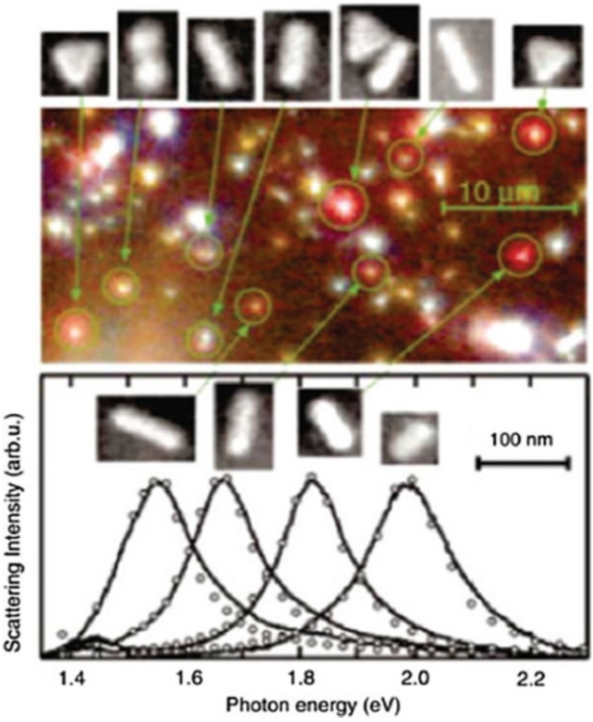

Fig. 1.3 Dark-field microscopy image, corresponding scanning electron microscopy images, and light-scattering spectra of Au nanocrystals of different shapes (Reprinted with permission from Ref. [34]. Copyright 2003 American Institute of Physics)

aperture, breaking the diffraction barrier of light [35–38]. However, for conventional aperture-type NSOM, the resolution is limited by the aperture size of the tip. Since the effective transmission area decreases as the fourth power of the aperture diameter [39, 40], the resolution improvement comes at the price of a sharp decrease in signal-to-noise ratio and contrast of NSOM images. Recently, differential near-field scanning optical microscopy (DNSOM) is introduced to improve the light transmission, which involves scanning a rectangular (e.g., a square) aperture (or a detector) in the near-field of the object of interest and recording the power of the light collected from the rectangular structure as a function of the scanning position [41].

Electron energy loss spectroscopy (EELS) is another powerful method for near-field mapping of LSPRs. When a material is exposed to a beam of electrons with a narrow range of kinetic energies, the constituent atoms can interact with these electrons via electrostatic (Coulomb) forces, resulting in elastic and inelastic scattering of electrons. Among them, inelastic scattering is associated with the energy loss of electrons, which can be measured via an electron spectrometer and interpreted in terms of what caused the energy loss [42]. EELS is a very powerful probe for the excitation on the surface and ultrathin films, in particular, for the collective excitations of electron oscillations (plasmons). Plasmon excitations are directly related to the band structure and electron density in a small volume of the particle probed by the focused electron beam [43]. With the recent proliferation of

aberration-corrected and monochromated transmission electron microscopes (TEMs), mapping the energy and spatial distribution of metallic nanoparticle plasmon modes on nanometer-length scales using EELS has become possible [44–47]. For example, Liz-Marzan and coworkers utilized a novel method relied on the detection of plasmons as resonance peaks in EELS to record maps of plasmons with sufficiently high resolution to reveal the dramatic spatial field variation over silver nanotriangles [48]. The near-field plasmon modes of isolated and coupled Au nanorods have also been imaged using EELS and energy-filtered transmission electron microscope (EFTEM) [49]. More recently, plasmon mapping of a series of high-aspect-ratio Ag nanorods using EELS was also reported [50]. These data indicate that correlated studies will ultimately provide a unified picture of optical and electron beam-excited plasmons and reinforce the notion that plasmon maps derived from EELS have direct relevance for the plethora of processes relying on optical excitation of plasmons.

The local field enhancements on the surface of nanoparticles arising from plasmonic excitations can also be indirectly probed by surface-enhanced spectroscopies. For example, the local field enhancements provide well-defined "hot spots" for surface-enhanced Raman scattering (SERS) [51–54]. Once the molecules get into these hot regions in vicinity to a metallic nanostructure, their spectroscopic signals can be dramatically amplified. It has been demonstrated that SERS enhancements are dependent on the fourth power of the local field enhancements. Therefore, the Raman enhancements of the probing molecules in close proximity to a metal nanostructure provide a way to evaluate the local field enhancements. Since Raman enhancements are sensitively dependent on the distance between molecules and metal surfaces, one can smartly construct molecular rulers to map out the local field enhancement profiles surrounding a nanoparticle based on SERS [55].

4.3 Simulations of LSPRs

The most commonly used theoretical methods for the modeling of the LSPRs of metallic nanoparticles include both analytical and numerical methods [56–59]. The analytical methods are either derived from Mie scattering theory for spheres or from the quasi-static (Gans) model as applied to spheroids. Most popular numerical methods for electrodynamics simulations include the discrete dipole approximation (DDA), the finite-difference time-domain (FDTD) method, the finite element method (FEM), and boundary element method (BEM).

It was realized almost a century ago that classical electromagnetic theory (i.e., solving Maxwell's equations for light interacting with a particle) based on Mie scattering theory provides a quantitative description of the scattering and absorption spectra of spherical nanoparticles. However, Mie's work is incapable of addressing shape effects. Although the quasi-static approximation developed later is an alternative to elucidate the optical properties of spheroids, the solution is even harder to use because of frequency-dependent dielectric functions included in Maxwell's

equations. Meanwhile, the numerical methods for solving Maxwell's equations come in many different flavors. For example, the discrete dipole approximation (DDA) is a frequency domain approach that approximates the induced polarization in a complex particle by the response of a cubic grid of polarizable dipoles. The finite different time domain (FDTD) method can be applied in both two and three dimensions, in which a clever finite differencing algorithm is applied to Maxwell's equation by Yee [60], using grids for the electric field **E** and magnetic field **H**, which are shifted by half a grid spacing relative to each other. Using the finite element method (FEM), the solutions to Maxwell's equations are expanded in locally defined basis functions chosen such that boundary conditions are satisfied on the surfaces of the elements. Boundary element method (BEM) is another numerical computational method of solving linear partial differential equations which have been formulated as integral equations. These numerical methods have been shown to be capable of simulating both the far-field and near-field plasmonic properties of metallic nanostructures of almost arbitrary structural complexity.

In addition to the analytical and numerical methods mentioned above, the time-dependent density functional theory (TDDFT) is one of the most convenient approaches for the fully quantum mechanical calculations of the optical properties of metallic nanoparticles [61–63]. TDDFT, an extension of density functional theory (DFT) with conceptual and computational foundations analogous to DFT, is to use the time-dependent electronic density instead of time-dependent wave function to derive the effective potential of a fictitious noninteracting system which returns the same density as any given interacting system.

Combined experimental and theoretical efforts over the past two decades have shed light on the interesting geometry dependence of plasmonic properties of metallic nanoparticles with increasing geometric complexity. In the following section, before moving onto those more complicated nanoparticle geometries, we will start from the simplest geometry, a nanosphere, to demonstrate how the LSPRs can be systematically tuned by changing the compositional and geometric parameters of the nanosphere.

5 LSPRs of Metallic Nanospheres

5.1 LSPRs of Single-Component Nanospheres

Strong optical scattering and absorption of light by noble metal nanospheres in visible spectral region due to LSPRs are a classical electromagnetic effect, which was described theoretically by Mie in 1908 by solving Maxwell's equations. Mie's theory is most useful in describing the plasmonic properties of metallic particles that are spherically symmetric. Mie scattering theory is the exact solution to Maxwell's electromagnetic-field equations for a plane wave interacting with a homogeneous sphere of radius R with the same dielectric constant as bulk metal. The extinction cross section of the spheres can be obtained as a series of multipolar oscillations if the boundary conditions are specified. Therefore, the

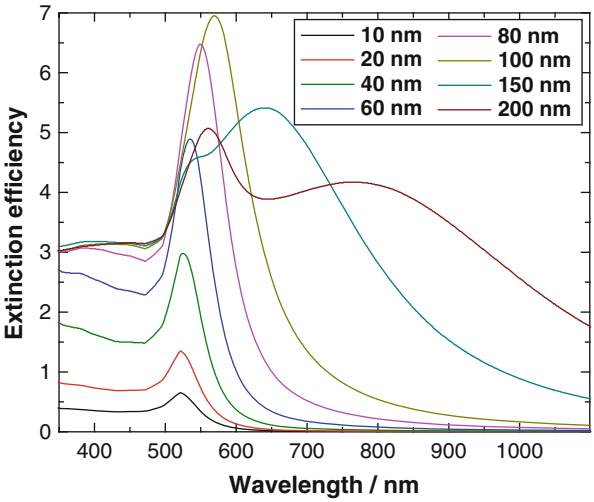

Fig. 1.4 Extinction spectra calculated using Mie scattering theory for Au nanospheres with diameters ranging from 10 nm to 200 nm dispersed in water. The calculated extinction is expressed as an efficiency, which is the ratio of the energy scattered or absorbed by the particle to the energy incident on its physical cross section

electrodynamics calculations can be simplified by only focusing upon low-order plasmon oscillations when the diameter of the spherical particle is much smaller than the wavelength of the radiation (within the quasi-static limit) and only dipole oscillation ($l = 1$) contributes to the extinction cross section which is a sum of both scattering and absorption. Based on this, the most popular form of Mie's theory for spherical nanoparticles within quasi-static limit is given as

$$C_{ext} = \frac{24\pi^2 R^3 {\varepsilon_m}^{3/2}}{\lambda} \bullet \frac{\varepsilon_2}{(\varepsilon_1 + 2\varepsilon_m)^2 + {\varepsilon_2}^2} \tag{1.2}$$

where C_{ext} is the extinction cross section of the spheres, ε_m is the dielectric constant of the surrounding medium, λ is the wavelength of the radiation, R is the radius of a homogeneous sphere, and ε_1 and ε_2 denote the real and imaginary part of the complex dielectric function of the particle material, respectively. A resonance occurs whenever the condition of $\varepsilon_1 = -2\varepsilon_m$ is satisfied, which explains the dependence of the LSPR extinction peak on the surrounding dielectric environment. It is this LSPR peak that accounts for the brilliant colors of a wide variety of metallic nanoparticles. The imaginary part of the dielectric function also plays a role in the plasmon resonance, relating to the damping, that is, resonance peak broadening in the spectrum.

For a small Au nanosphere within the quasi-static limit, its LSPR has an almost fixed resonance frequency and shows limited tunability. As shown in Fig. 1.4, the extinction spectra calculated using Mie theory for Au nanospheres smaller than 100 nm show that LSPR peaks are located in the green part of the visible region. According to the full Mie-theory solution, a limited red shift of LSPR wavelength and broadening of the resonant line shape appear as Au nanospheres progressively become larger within the sub-100-nm-size regime. As the particle size further

increases to the size regime beyond the quasi-static limit, the overall spectral line shape becomes more complicated as the higher-order multipolar resonances, such as quadrupole ($l = 2$) and octupole ($l = 3$), become increasingly significant in the extinction spectra in addition to the dipolar plasmon resonances due to the phase-retardation effects, resulting in further redshifted and broadened dipolar plasmon bands. Such size dependence of LSPRs has been experimentally observed to be in very good agreement with Mie scattering theory calculations for Au and Ag spherical or quasi-spherical particles over a broad size range both within and beyond the quasi-static limit [64, 65].

5.2 Effects of Materials' Electronic Properties on LSPRs of Nanospheres

In addition to the particle size, the frequencies of LSPRs of a nanosphere also rely on the electronic properties of the constituent materials. The LSPR frequency, although tunable by varying the nanoparticle size and local medium, is primarily controlled through the free electron density (N) of the material. Although LSPRs typically arise in nanostructures of noble metals, they are not fundamentally limited to noble metals and can also occur in other non-noble metals, conducting metal oxides and semiconductors with appreciable free carrier densities. Recently, Alivisatos and coworkers demonstrated that in analogy to noble metal nanoparticles, doped semiconductor quantum dots may also exhibit LSPRs whose resonance frequencies can be tuned by controlling the free carrier densities of the materials [66]. Figure 1.5 depicts the modulation of the LSPR frequency (ω_{sp}) of a spherical nanoparticle within the quasi-static limit through control over its free carrier concentration (N). In this figure, the LSPR frequency can be estimated using the following equation:

$$\omega_{SP} = \frac{1}{2\pi}\sqrt{\frac{Ne^2}{\varepsilon_0 m_e(\varepsilon_\infty + 2\varepsilon_m)}} \tag{1.3}$$

Here the high frequency dielectric constant (ε_∞) is assumed to be 10, the medium dielectric constant ε_m is set as 2.25 for toluene, and the effective mass of the free carrier m_e is assumed to be that of a free electron. e is the electronic charge, and ε_0 is the permittivity of free space. The top panel shows a calculation of the number of dopant atoms required for nanoparticle sizes ranging from 2 to 12 nm to achieve a free carrier density between 10^{17} and 10^{23} cm^{-3}. To achieve LSPRs in the visible region, a metallic material in which every atom contributes a free carrier to the nanoparticle is required. For LSPRs in the infrared, carrier densities of 10^{19}–10^{22} cm^{-3} are required. Below 10^{19} cm^{-3}, the number of carriers (for a 10-nm nanocrystal) may be too low (<10) to support an LSPR mode.

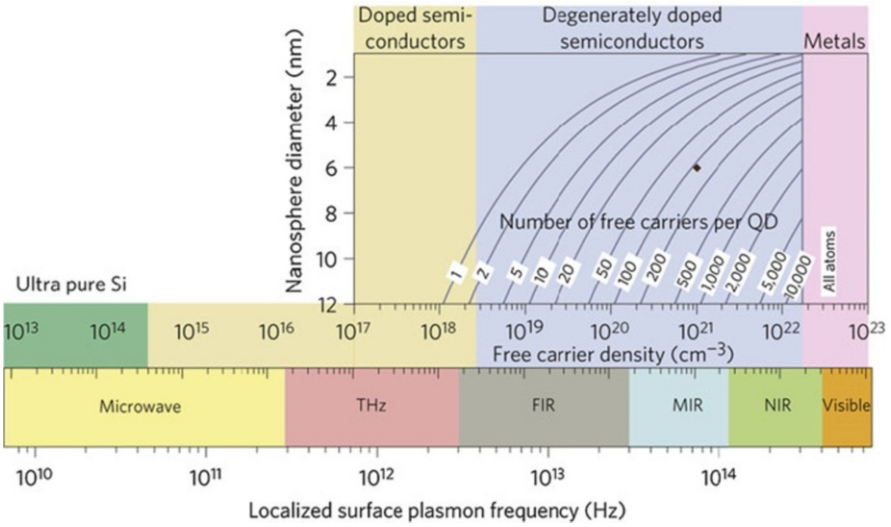

Fig. 1.5 LSPR frequency dependence on free carrier density and doping constraints (Reprinted with permission from Ref. [66]. Copyright 2011 Nature Publishing Groups)

The most commonly studied plasmonic materials so far are noble metals, such as Au, Ag, and Cu, which have free electron densities in the range of 10^{22}–10^{23} cm^{-3} with corresponding LSPRs in the visible. For non-noble metals, such as Pb, In, Hg, Sn, Cd, and Al, their LSPR frequencies lie in the UV region of the spectrum, and nanoparticles do not display well-defined LSPR bands that are as tunable as those of the noble metals. In addition, small particles of these non-noble metals are also chemically unstable and readily oxidized, making it difficult to measure their LSPRs. The LSPRs of doped semiconductor nanoparticles typically occur in the infrared and are not as strong and well-defined as those of noble metal nanoparticles. The geometry dependence of LSPRs of doped semiconductor nanoparticles is still poorly understood at the present stage. Therefore, we will only focus on the plasmonic properties of noble metal nanoparticles, Au and Ag nanoparticles in particular, because of not only their relatively high chemical and photostability but also more importantly their intense and geometrically tunable LSPRs across the visible and NIR regions.

In addition to the free electron densities of the materials, the optical properties of noble metal nanospheres are also strongly influenced by the electronic band structures of the constituent metal, which determine the metal's dielectric functions. The complex dielectric function of a material, denoted as $\varepsilon = \varepsilon_1 + i\varepsilon_2$, describes a material's response to an applied electric field. ε_1 determines the degree to which the material polarizes in response to an applied field, while ε_2 controls the relative phase of this response with respect to the applied field. Intrinsic loss mechanisms (e.g., electron scattering) of a material are all

condensed into ε_2. For the noble metals at optical frequencies, the dielectric function can be expressed as the sum

$$\varepsilon(m) = 1 + \chi_\infty + \chi_D(\omega) \tag{1.4}$$

where the background susceptibility χ_∞ arises from the core electron polarizability and interband (d → sp) transitions and χ_D is the Drude response of the conduction electrons. The background polarizability and free space response are often combined into $\varepsilon_\infty = 1 + \chi_\infty$ In the Drude model [30],

$$\chi_D(\omega) = -\frac{\omega_P^2}{\omega^2 + i\Gamma\omega} = -\frac{\omega_p^2}{\omega^2 + \Gamma^2} + i\frac{\omega_p^2\Gamma}{\omega(\omega^2 + \Gamma^2)} \tag{1.5}$$

where ω_P is the bulk plasmon frequency and Γ is the reciprocal electron relaxation time. In the visible and NIR, $\Gamma << \omega$; therefore,

$$\chi_D(\omega) \cong -\frac{\omega_P^2}{\omega^2} + i\frac{\omega_p^2}{\omega^3}\Gamma \tag{1.6}$$

To completely understand the role that the metal plays in determining the optical properties of metallic nanoparticles, it is necessary to examine and account for the effects of both the free-electron and electronic interband transition contributions to the metal's dielectric response. Figure 1.6 shows a comparison of dielectric functions of Ag, Au, and Cu, together with the calculated extinction spectra of Au, Ag, and Cu nanospheres that are 30 nm in diameter obtained using Mie scattering theory. The dielectric medium surrounding the nanoparticles is water. The spectral regions where interband transitions occur are shaded in green. The onset of electronic interband transitions from the valence band to the Fermi level causes a sharp increase in the imaginary part (ε_2) and a marked change in the slope of the real part (ε_1) of the dielectric functions. For 30-nm-diameter solid nanospheres, the relative spectral locations of the particle plasmon resonance and the constituent metal's interband transitions determine the nanoparticles' optical response, resulting in significant variations between Au, Ag, and Cu nanospheres. The Ag nanosphere has by far the strongest plasmon resonance because of the higher energy of the interband transitions (~3.8 eV), relative to the energy of the plasmon resonance, resulting in minimal damping of the plasmon. The Au nanosphere displays a well-defined plasmon resonance at ~520 nm, which is closer to the edge of the interband transitions region (~2.5 eV) than the case of Ag. With plasmon resonant energies well below the interband transitions, Au and Ag nanoparticles can be treated as free-electron systems whose optical properties are determined by the conduction electrons, with only a constant real background polarizability associated with the core electrons. The Cu nanosphere, however, has much weaker optical response in comparison to Ag and Au due to the nanosphere plasmon being resonant with the interband transition region (~2.1 eV)

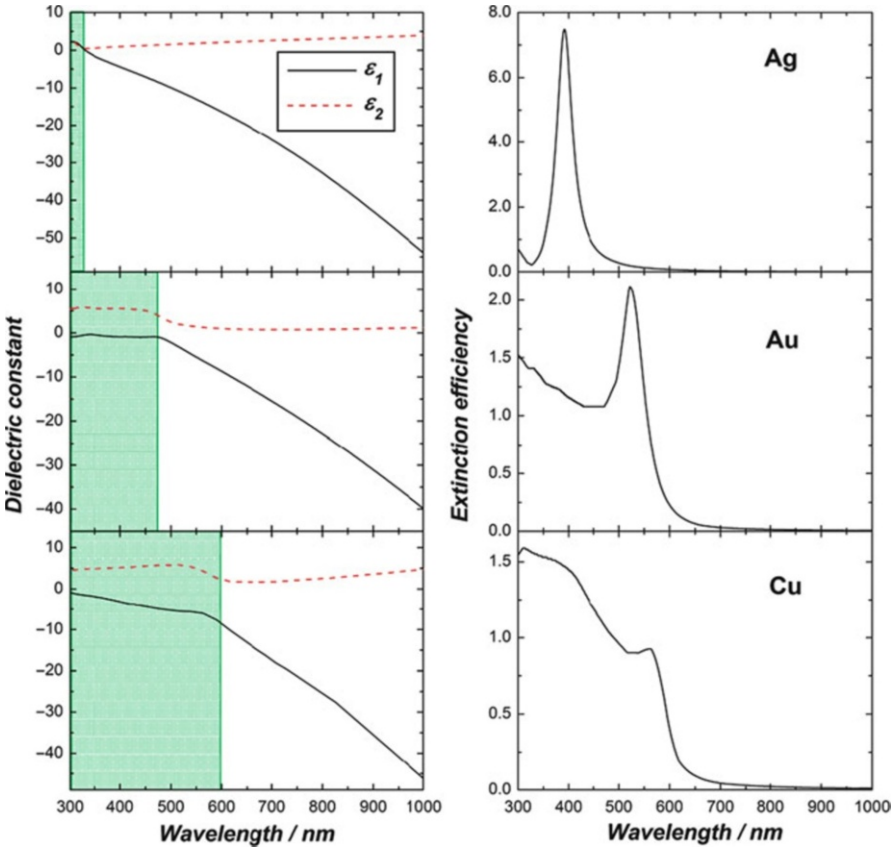

Fig. 1.6 Dielectric functions (*left column*) and calculated extinction spectra of a 30-nm-diameter nanosphere (*right column*) of Ag (*top*), Au (*middle*), and Cu (*bottom*)

of the spectrum. The interband transitions are responsible for a strong damping of the Cu nanosphere plasmon and the strong "background" absorption on top of which a weak plasmon resonance peak is visible.

5.3 Bimetallic Nanospheres

When multiple metallic components are integrated into one nanosphere, the resulting optical properties become dependent upon both the compositions and the compositional distribution inside the nanoparticle. Although various bimetallic nanoparticle systems have been studied, combinations of Au and Ag are of particularly interest largely for two reasons. First, both metals display intense and well-defined LSPR bands in the visible at around 400 and 520 nm for spherical nanoparticles of Ag and Au, respectively. Second, both Au and Ag form

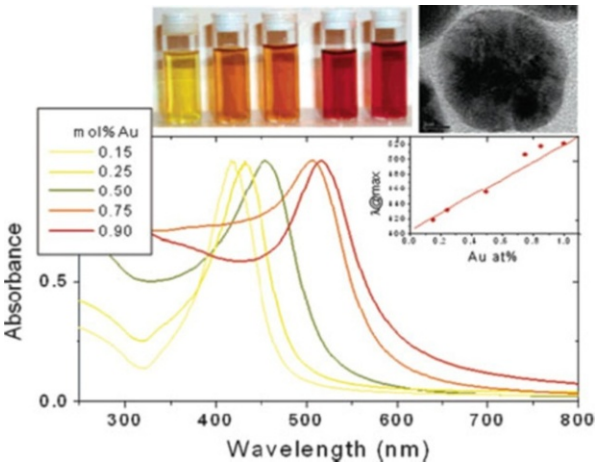

Fig. 1.7 UV–visible spectra of Au–Ag alloy nanoparticle colloids with varying compositions. A linear fit of the peak position of the experimental absorption band as a function of composition obtained using Mie theory is plotted (*inset*). HRTEM image shows the homogeneous distribution of Au and Ag atoms within the particles (Reprinted with permission from Ref. [80]. Copyright 2006 American Chemical Society)

face-centered cubic crystalline structures with very small lattice mismatch (lattice constants of 4.078 Å and 4.086 Å for Au and Ag, respectively), and therefore, they can form heteronanostructures through epitaxy growth or form alloy nanostructures with various compositional stoichiometries. Spherical nanoparticles of Au–Ag alloy [67–73], Au–Ag core–shell [74–78], and Ag–Au core–shell [74, 79] have been fabricated through various bottom-up chemistry approaches. Precise control over both the compositional stoichiometry and distribution enables one to systematically study the interesting optical tunability of bimetallic nanospheres.

For alloy nanospheres normally prepared by simultaneous reduction of the metal salts, it has been observed that the plasmon band of the alloy nanoparticles lies somewhere between those for pure Ag and pure Au nanoparticles [70, 71], and there is a linear relationship between the compositional stoichiometry and the wavelength of the plasmon band of the alloy particles. As shown in Fig. 1.7, a continuous color evolution from yellow to red can be clearly observed as the Au to Ag ratio progressively increases [80]. As shown in the inset plots of Fig. 1.7, the experimentally observed linear relationship between compositional stoichiometry and LSPR wavelength can be well reproduced by Mie scattering theory calculations. The LSPR shifts were initially modeled by assuming a linear combination of the dielectric functions of pure Au and Ag as input for the Mie scattering theory calculations, but El-Sayed and coworkers have demonstrated that the theoretical predictions agreed with the experimental results more accurately when experimentally measured dielectric functions for Au–Ag alloy films were used. The linear relationship between compositional stoichiometry and wavelength of LSPR band applies to alloy nanoparticles only and cannot be simply extended to core–shell heterostructured nanoparticles.

Core–shell heterostructured bimetallic nanoparticles can be fabricated either via segregation during simultaneous reduction or by successive reduction of the

different metals [68, 81, 82]. Recently, the creation of onion-like multilayer bimetallic nanoparticles obtained by successive reduction of $AgNO_3$ and $HAuCl_4$ with ascorbic acid in the presence of cetyltrimethylammonium bromide (CTAB) has been reported. The optical properties of these core–shell bimetallic nanoparticles are quite sensitive to the multilayer deposition, and the extinction spectral line shape are mostly dominated by the geometry of the outermost layer [83]. It is interesting that the core–shell heterostructured bimetallic nanoparticles may undergo alloying processes under appropriate conditions. For Au–Ag bimetallic nanoparticles, the core–shell heterostructures may be kinetically favorable during the particle formation, while the alloy particles are thermodynamically more stable. Therefore, the transitions from the core–shell heterostructures to alloy homostructures are in principle spontaneous at room temperature. By modifying the experimental conditions, such transitions may be accelerated and kinetically better controlled. For example, Hartland and coworkers [75] used nanosecond and picosecond lasers to melt the Au–Ag core–shell particles into homogeneously alloyed nanoparticles. Sun and coworkers [79] reported the formation of monodisperse Au–Ag alloy nanoparticles through interface diffusion of Ag–Au core–shell nanoparticles under solvothermal conditions in organic solvents. Recently, Tracy and coworkers [84] reported a facile method for the synthesis of Au–Ag core–shell nanoparticles and their subsequent transition to Au–Ag alloy nanoparticles through digestive ripening. By controlling the relative sizes of the Au core and Ag shell, the stoichiometry of the resulting Au–Ag alloy nanoparticles can be precisely controlled. The structural change of the particles during the alloying processes can be monitored through the shift of the LSPR bands. Precise control over the particle's geometry and compositions is important to the fine-tuning of the optical properties of the bimetallic nanoparticles as their LSPRs are sensitively dependent on both the stoichiometry and geometrical distribution of the metal compositions.

6 LSPRs of Metallic Nanorods

6.1 Geometrically Tunable LSPRs of Nanorods

Metal nanorods are elongated, anisotropic nanoparticles with polarization-dependent response to the incident light. The excitation of the electron oscillation along the short axis induces a plasmon band at wavelength similar to that of Au nanospheres, commonly referred to as the transverse band. The excitation of the electron oscillation along the long axis induces a much stronger plasmon band in the longer wavelength region, referred to as the longitudinal band. When Au nanorods are dispersed in a solvent, a steady-state extinction spectrum containing both bands of longitudinal and transverse plasmons can be observed due to the random orientation caused by the continuous Brownian motion of the particles. While the transverse band is insensitive to the size of the nanorods, the longitudinal band is redshifted significantly from the visible to NIR region with increasing aspect ratio (length/width) [85–87].